

## On the retrieval of water vapour profiles from a single GPS station

M. CAPUTO<sup>(1)</sup>, V. RUGGIERO<sup>(1)</sup>, A. SUTERA<sup>(1)</sup> and F. ZIRILLI<sup>(2)</sup>

<sup>(1)</sup> *Dipartimento di Fisica, Università di Roma "La Sapienza" - Roma, Italy*

<sup>(2)</sup> *Dipartimento di Matematica, Università di Roma "La Sapienza" - Roma, Italy*

(ricevuto il 23 Marzo 2000; approvato il 14 Luglio 2000)

**Summary.** — In this paper we present an inversion method to retrieve atmospheric water vapour profiles from GPS signals received by a single station. The method uses a formula relating the refraction index to the delay time that includes the curvature effect of the signal path.

PACS 96.60.Jq – Water in the atmosphere (humidity, clouds, evaporation, precipitation).

PACS 93.85 – Instrumentation and techniques for geophysical research.

### 1. – Introduction

Climate is the end result of the complex interactions between radiation transfer in the atmosphere and the response of the dynamics to such an input. Knowledge of the processes leading to the establishment of this equilibrium will add confidence to our prediction of future climate variations whatever the causes of these variations might be: natural or man induced.

A simple analysis of the climate system leads to the recognition that radiatively active gases are important in determining the outgoing radiation. Among these gases water vapour plays the largest role in cooling the atmosphere so that the solar energy stored in the Earth surface can be redelivered out to space. This highly variable radiatively active substance strongly influences the radiative balance and the knowledge of its vertical distribution appears as the most important information needed to establish a correct radiative balance. Unfortunately, only very little information on the vertical distribution of water vapour is available. So that the retrieval of the vertical distribution of water vapour is one of the most challenging scientific endeavours in climate research.

Among the methods to measure the water vapour vertical distribution, one that appears promising, for its precision and for the relatively low cost, is the method provided by the signal of the Global Positioning System (GPS) satellites cluster as reported in G. Bevis *et al.* (1992).

High-accuracy GPS receivers are used commonly to monitor earthquake, or volcanic and tectonic processes with millimeter precision. To achieve this accuracy

scientists correct the GPS data to consider the GPS signal propagation effects of the charged ionosphere and the hydrostatic and wet delays of the electrically neutral atmosphere. With suitable ancillary information, the uncorrected GPS data can be used to estimate integrated precipitable water (IPW) and ionospheric total electron content (TEC) with impressive accuracy. The hydrostatic delay can be approximated closely using measurements of surface pressure and temperature at the receiver site. The ionospheric delay can be estimated from the dispersion relation between the two frequencies employed by the GPS satellites (in the GPS jargon L1 and L2). The delay remaining is attributable, to the effect of the stratification of the dry atmosphere and to the total-column of precipitable water.

The retrieval of vertical profiles of the water vapour is usually obtained with approaches different from the one proposed here; for example, the required information can be obtained by means of an occultation method once a GPS receiver is launched in space in a low orbit (see, for example, Hardy *et al.*, 1992).

In the present paper we explore the possibility of deriving information on the vertical structure of the water vapour from data collected in a GPS ground-based receiver. We believe that this is made possible by exploiting a formula which relates the delay of the GPS signal to the curved optical path and to the water vapour pressure. In sect. 2 we discuss the equation which will be used for the profile retrieval. In sect. 3 we present results obtained for simulated water vapour profiles assuming an exponential height dependence of the refraction index. In sect. 4 we remove the previous assumption and we solve the inverse problem with simulated data with no assumptions on the functional dependence of the refraction index from height. Finally in sect. 5 some conclusions are drawn.

## 2. – The time delay equation

Let  $c$  be the speed of light and  $n$  be the refraction index of the atmosphere, the radio signal speed in the atmosphere is given by

$$(1) \quad v = c/n .$$

Figure 1 shows the typical path of the signal going from the satellite to the receiver. Let  $s$  be the Earth radius, the vertical coordinate  $r$  is the height above the Earth surface given by  $r = s$ , the angle  $i$  is the local zenith angle. Assuming a plane parallel atmosphere  $n$  is just a function of height, that is  $n = n(r)$  for  $r \geq s$ .

The path curvature is due to the atmospheric stratification which allows, through Snell's Law, to relate  $n$  and  $i$  as follows.

Let  $dS$  be the infinitesimal element of the signal path, we have

$$(2) \quad dS = \frac{n(r) dr}{\cos(i(r))} ,$$

$$(3) \quad n(r) r \sin(i(r)) = n(s) s \sin(i(s)) ,$$

for any  $r \geq s$ .

From simple algebraic manipulations it is easy to see that the delay time introduced

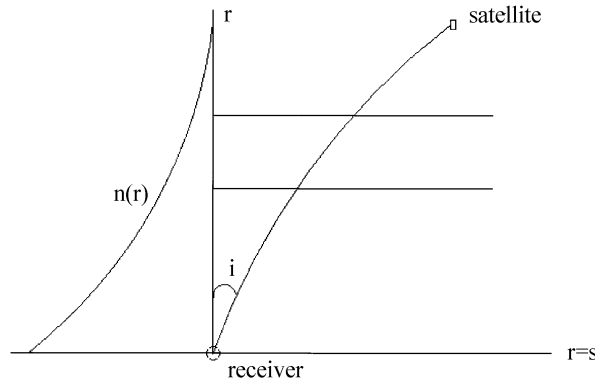


Fig. 1. – Signal propagation from satellite to station.  $r$  is in km,  $s$  dimensionless.

by the neutral atmosphere  $t(i(s))$  is given by

$$(4) \quad t(i(s)) = \int_s^R \frac{(1 + N(r) \cdot 10^{-6})}{c \sqrt{1 - \left( \frac{s(1 + N(s) \cdot 10^{-6}) \sin(i(s))}{r(1 + N(r) \cdot 10^{-6})} \right)^2}} dr,$$

where  $R$  is the top of the atmosphere that is 60 km above the Earth surface and we have used the definition

$$(5) \quad n(r) = 1 + N(r) \cdot 10^{-6}, \quad r \geq s.$$

Equation (4) can be regarded as an integral equation for the unknown  $N(r)$ ,  $s \leq r \leq R$  having the function  $t(i(s))$  as data.

On the other hand, we have

$$(6) \quad N = K_1 \frac{P}{T} + K_2 \frac{\bar{e}}{T^2},$$

where  $P$ ,  $T$ ,  $\bar{e}$  are the pressure, temperature and water vapour saturation pressure, respectively. The quantities  $K_1$  and  $K_2$  are known constants.

Given the function  $t(i(s))$ ,  $\alpha \leq i(s) \leq \beta$ , for a choice of the constants  $\alpha$  and  $\beta$ , the solution of the integral equation (4) gives  $N(r)$ ,  $s \leq r \leq R$  and eq. (6) makes it possible to derive the vertical profile of  $\bar{e}$  when  $P$  and  $T$  are known.

### 3. – Water vapour retrieval for a profile of a given functional form

As mentioned in the introduction, in this paper we analyse only simulated data. The simulated data are obtained as follows: the delay time  $t$  (in seconds) is obtained from a known profile  $N(r)$ ,  $s \leq r \leq R$  computing (4) using a quadrature formula. Then in order to simulate an actual experiment, we add to the computed delay time  $t$  a random number uniformly distributed in the interval  $(-3 \cdot 10^{-11} \text{ s}, 3 \cdot 10^{-11} \text{ s})$ .

To determine the known profile  $N(r)$ ,  $s \leq r \leq R$  used to simulate the delay times, we

TABLE I.

Atmosphere	$N(s) \cdot 10^{-6}$	True value of $H$ (km)	Found value of $H$ (km)
MLS	343.1	7.76	7.80
MLW	312.4	8.10	8.14
SAS	324.6	7.94	7.98
SAW	314.1	8.05	8.09
TROPICAL	361.5	7.61	7.65

proceed as follows: we choose the typical values of  $T$ ,  $P$  and  $\bar{e}$  for an averaged atmosphere at different latitudes and seasons. These values are some of the profiles usually adopted to test radiative transfer models as described, for example, in Ellingson and Fouquart (1991). The refraction index  $N$  is finally determined by fitting a decreasing exponential of the form (7) in eq. (6) with the constraint that  $\bar{e}(r) > 0$ ,  $r > s$ .

With applications in mind in the reconstruction procedure, we have assumed  $N$  known at the Earth surface, that is  $N(s)$  is known.

In this section we attempt to recover  $N$  making the assumption that

$$(7) \quad N(r) = N(s) e^{-r/H}, \quad s \leq r \leq R,$$

where  $H$  is the unknown height scale that must be determined using (4).

The results of the inversion procedure are shown in table I for the midlatitude summer (MLS), midlatitude winter (MLW), subartic summer (SAS), subartic winter (SAW) and tropical atmosphere profiles, respectively.

The corresponding water vapour profiles are shown in fig. 2a)-e).

Moreover, using the method outlined above we have calculated the water vapour profile leaving unknown both the surface value of the refraction index and the height scale in the exponential (7) for the NCAA standard atmosphere. The results are shown in table II while the corresponding profile of  $\bar{e}$  is presented in fig. 3.

These results show how the small angle dependence of  $t$  can be successfully exploited to determine the water vapour pressure when data of sufficient quality are available. It may be thought that the random error added to the numerically computed delay in this paper is too small compared to the actual errors present in the physical measurements. However, considering that more than one satellite is in the field of view of the receiver, we believe that the error can be reduced to the size considered here by interpolation procedures.

TABLE II.

True value of $N(s) \cdot 10^{-6}$	True value of $H$ (km)	Found value of $N(s) \cdot 10^{-6}$	Found value of $H$ (km)
315.0	7.36	314.3	7.37

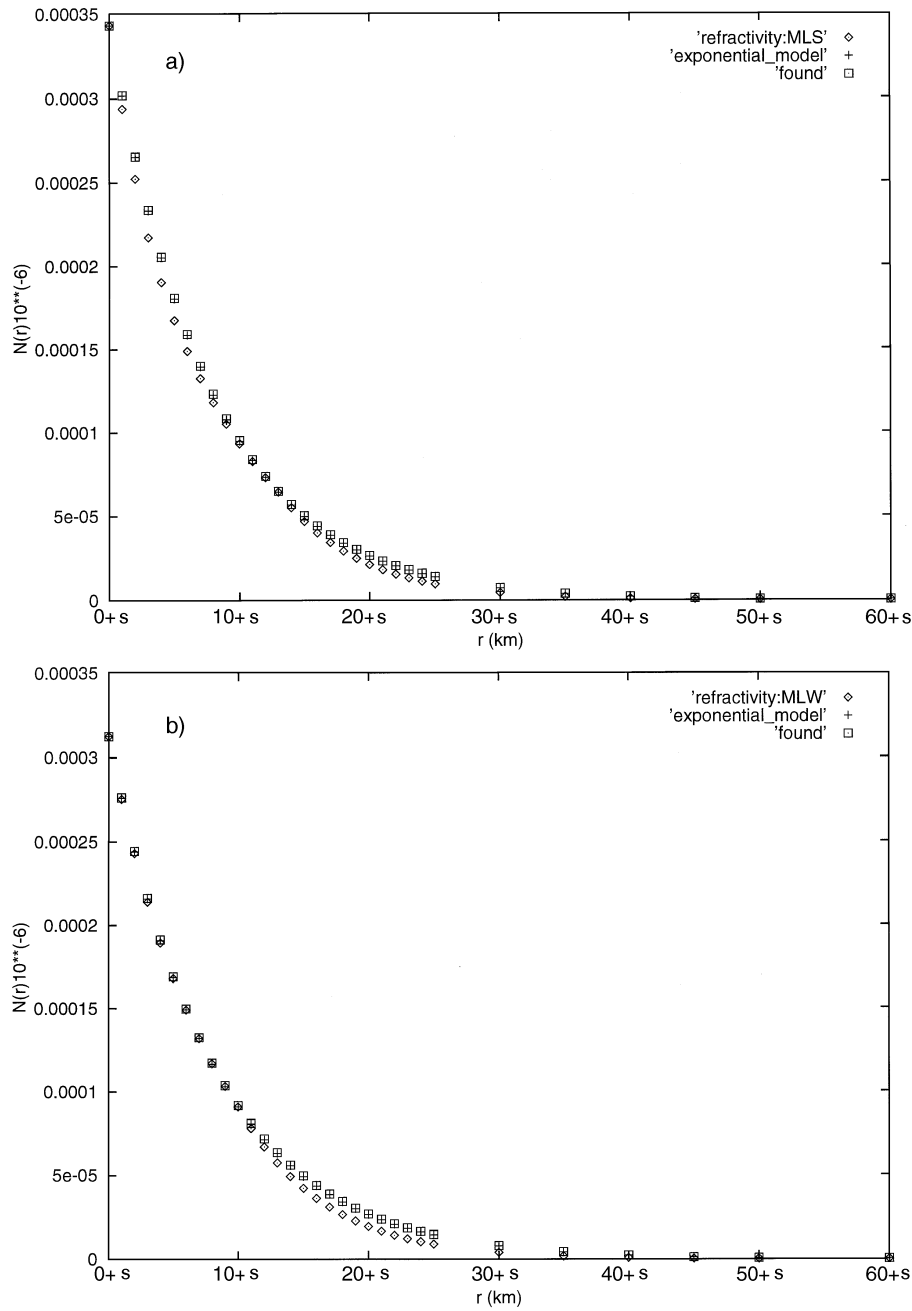


Fig. 2. – a) Comparison between water vapour pressure midlatitude summer model (diamonds), water vapour pressure exponential version midlatitude summer model (crosses), water vapour pressure found by the retrieval procedure (squares). b) Comparison between water vapour pressure midlatitude winter model (diamonds), water vapour pressure exponential version midlatitude winter model (crosses), water vapour pressure found by the retrieval procedure (squares).

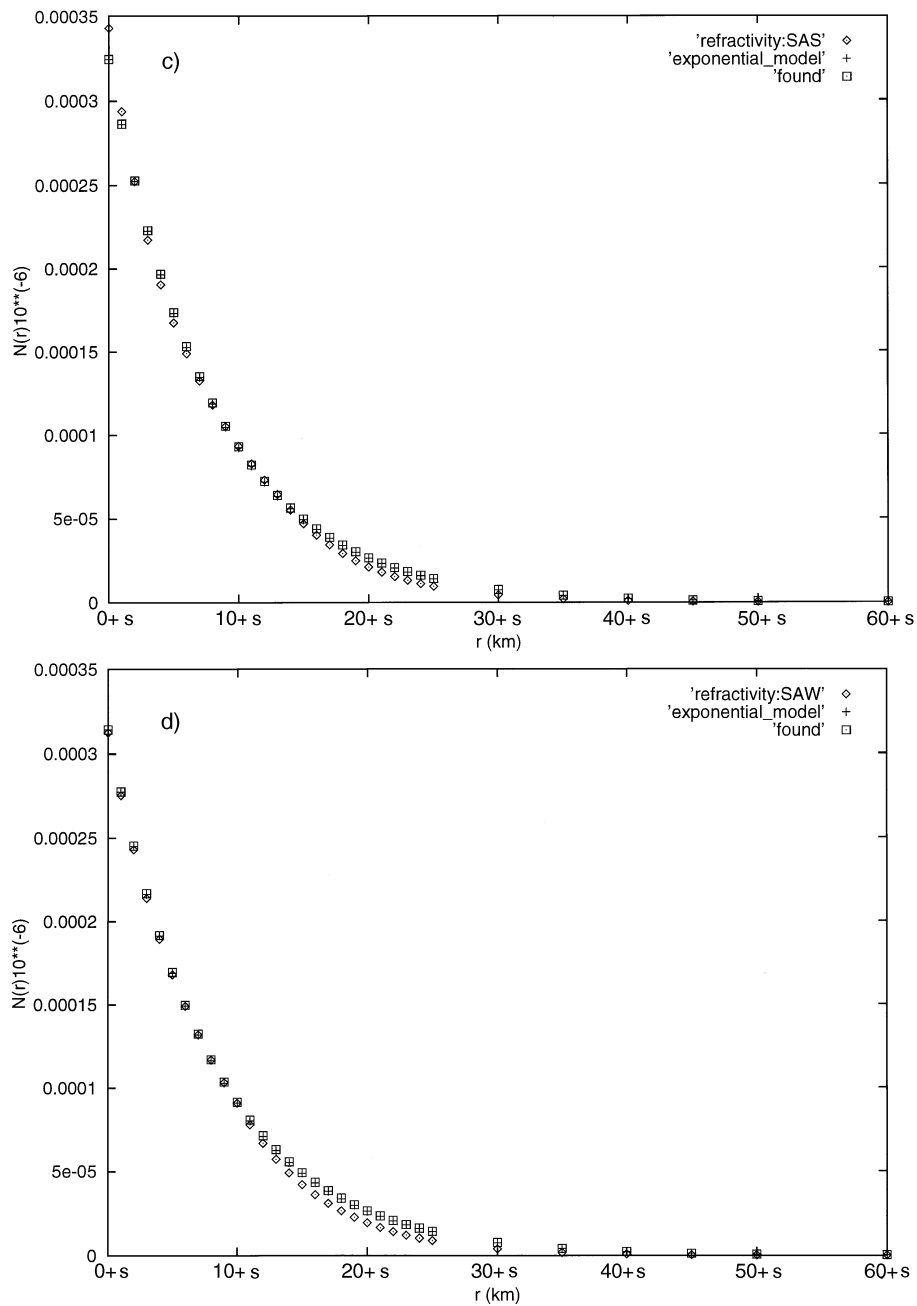


Fig. 2. (continued) – c) Comparison between water vapour pressure subartic summer model (diamonds), water vapour pressure exponential version subartic summer model (crosses), water vapour pressure found by the retrieval procedure (squares). d) Comparison between water vapour pressure subartic winter model (diamonds), water vapour pressure exponential version subartic winter model (crosses), water vapour pressure found by the retrieval procedure (squares).

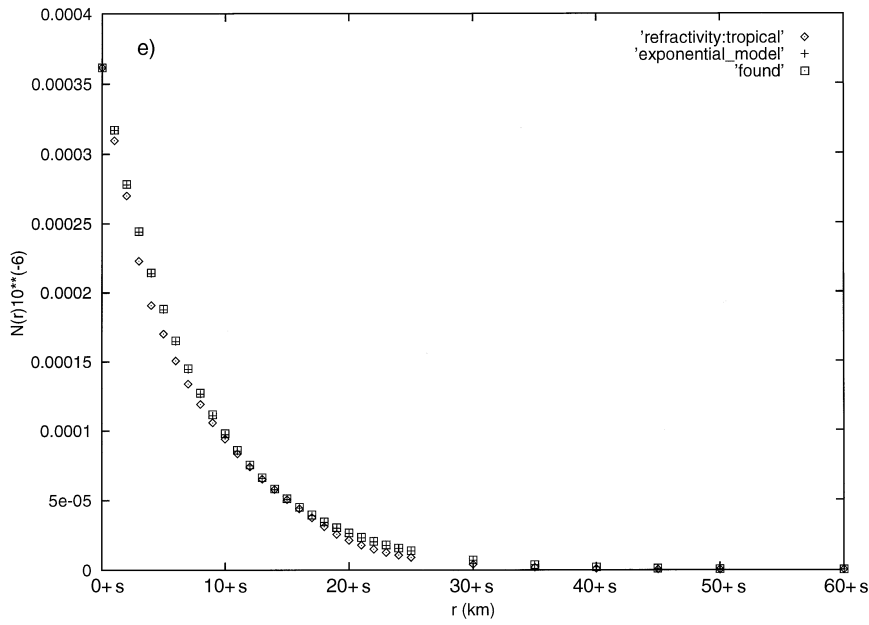


Fig. 2. (continued) – e) Comparison between water vapour pressure tropical model (diamonds), water vapour pressure exponential version tropical model (crosses), water vapour pressure found by the retrieval procedure (squares).

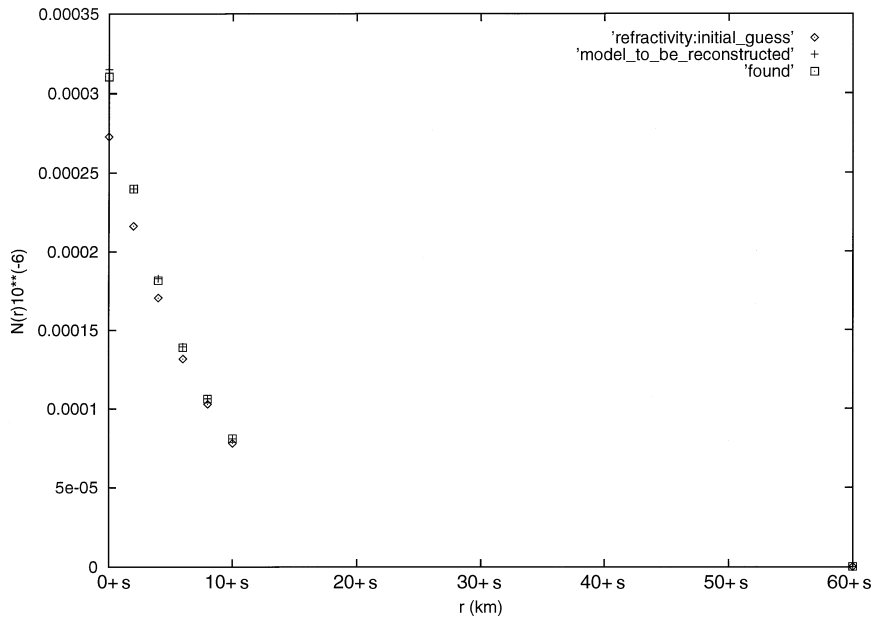


Fig. 3. – Comparison between water vapour pressure initial guess (diamonds), water vapour pressure to be reconstructed (crosses), water vapour pressure found by the retrieval procedure (squares).

#### 4. – An inversion algorithm

The previous section has shown a good agreement between fitted and reconstructed profiles. However, when we compare the  $\bar{e}$  profiles with the observed ones we notice relevant discrepancies. This is due to our assumption about the functional (exponential) dependence of  $N$  with height. Analysing the data in more detail, it appears that such an assumption is too coarse a representation of the data.

In this section we remove this assumption by inverting (4) with no further constraints.

Let  $t(i_k(s))$ ,  $k = 1, 2, \dots, M$  be the known delay time measurements. We choose the nodal points  $r_k$ ,  $k = 1, 2, \dots, L$  and the corresponding unknowns  $N_k$ ,  $k = 1, 2, \dots, L$  that are approximations of  $N(r_k)$ ,  $k = 1, 2, \dots, L$ , respectively. We always assume  $L \leq M$ . The integral in (4) is approximated by using a quadrature rule having  $r_k$ ,  $k = 1, 2, \dots, L$  as nodal points and the unknown quantities  $N(r_k)$ ,  $k = 1, 2, \dots, L$  substituted with their approximated values  $N_k$ ,  $k = 1, 2, \dots, L$ . The simplest quadrature rule is the rectangular rule, however, when useful, higher-order formulae may be used.

Let  $\vec{r} = (r_1, r_2, \dots, r_L)$ ,  $\vec{N} = (N_1, N_2, \dots, N_L)$  be two vectors and let  $Q(\vec{r}, \vec{N}, i(s))$  be the approximation of the integral in (4) obtained using the quadrature rule chosen. The solution of the integral equation (4) in the unknown  $N(r)$  is translated in the following nonlinear least-squares problem: given  $t(i_k(s))$ ,  $k = 1, 2, \dots, M$  and  $\vec{r}$

$$(8) \quad \underset{\vec{N}}{\text{minimize}} \sum_{k=1}^M (t(i_k(s)) - Q(\vec{r}, \vec{N}, i_k(s)))^2.$$

For physical reasons, the constraints  $N_k \geq 0$ ,  $k = 1, 2, \dots, L$  must be enforced when solving the minimization problem (8).

We seek a global minimizer of (8). In our experience (8) is very ill conditioned. The numerical algorithm used to solve (8) is a simple adaptation of the algorithm SIGMA proposed in Aluffi-Pentini *et al.* (1988a, b) and is based on the numerical solution of the Cauchy problem for a stochastic differential equation. The choice of the stochastic differential equation is inspired by statistical mechanics.

Employing the algorithm described above, we have reconstructed  $\vec{N}$  and from  $\vec{N}$ , using (6), we have obtained the water vapour profile for the case of a standard atmosphere.

TABLE III. –  $N_{( )}$  is the refraction index (0 initial guess, f found value, s true value),  $e_{( )}$  is the water vapour pressure (f found value, s true value).

Height (km)	$N_0(r) \cdot 10^{-6}$	$N_f(r) \cdot 10^{-6}$	$e_f(r)$ (mb)	$N_s(r) \cdot 10^{-6}$	$e_s(r)$ (mb)
0	272.8	310.3	8.33	315.0	9.37
2	216.3	239.9	5.14	240.0	5.16
4	170.6	181.6	2.02	162.9	2.26
6	131.6	138.8	1.25	139.4	1.35
8	102.7	106.1	0.54	106.2	0.56
10	78.0	81.1	0.45	80.9	0.42
60	0.06	0.10	$5.8 \cdot 10^{-3}$	0.09	$4.28 \cdot 10^{-3}$



TABLE IV. –  $N_{(j)}$  is the refraction index (0 initial guess, f found value, s true value).

Height (km)	$N_0(r) \cdot 10^{-6}$	$N_f(r) \cdot 10^{-6}$	$N_s(r) \cdot 10^{-6}$
2	218.2	237.3	252.2
4	178.3	186.1	190.3
6	144.6	145.9	148.8
8	116.3	116.3	117.9
10	92.6	93.1	93.2
60	0.02	0.76	0.14

The initial guess chosen to start the minimization procedure corresponds to a dry atmosphere.

Dividing the domain in five equally deep layers for the troposphere and one layer covering the rest of the atmosphere, we get the results summarized in table III.

The estimated water vapour has an error that does not exceed 8% over all the column, which may be considered well within the range of measurement errors for this variable both with the traditional sensors or with more sophisticated apparatus such as Raman lidars. This is true in particular for the upper levels of the atmosphere.

We argue that this retrieval result adds important information to the knowledge of the upper-troposphere water content, which is well known to be a crucial variable to estimate atmospheric cooling rates and to calculate the earth radiation budget on climatic time scales (see, for example, Harries, 1996). Similar information may be obtained only on a global scale with a rather expensive experimental network.

Next we consider the effect of a random error on a refraction index profile. The error is introduced in the manner discussed in the previous section.

As an example, we used the middle-latitude summer atmosphere to compute an exponential refraction index. The surface refraction index is kept fixed to the value suggested by  $\bar{e}$ ,  $T$  and  $P$  of the atmosphere considered.

The layer depths have been chosen as described above. The results are shown in table IV.

We can see that the solution approximates closely the refraction index generating the simulated data.

## 5. – Conclusions

In fig. 2a)-e) we note that beginning at an elevation of about 10 km there is a remarkable difference between the standard water vapour profile (diamonds) and the profile found (crosses) which increases with height reaching a maximum of about 1 mbar, at a height of about 15–25 km, depending on the latitude and the season.

Since the water vapour pressure standard profile is not necessarily exponential, also the corresponding refraction index profile used in the inversion procedure is not necessarily exponential. That is from the inversion procedure we may expect a nonexponential profile of the refraction index which in turn gives a nonexponential profile of the water vapour content. The difference between the water vapour content standard profile and its exponential approximation accounts for about 0.25 mbar which is a quantity of the same order of the difference between the values of the standard

profile and the profile found using the inversion procedure. The difference between the water vapour standard profile and its exponential approximation could therefore have some relevance to explain the difference between the profile found and the standard one and may have relevant consequences on the accuracy of the profile found.

We note that the water vapour content varies the season and the latitude. The variation with height is irregular; for instance, in fig. 2d, it is shown that, at 15 km height, we have 60% of the maximum value of the water vapour of the standard model. The last value is recorded at a height of about 2 km, where the vapour water content is about 35% greater than at the surface.

Finally, we note also that in all cases considered, the water vapour content has a minimum at a height of about 10 km and a maximum between 15 and 25 km depending on latitude and season. The latter phenomena call for the definition of a sort of bimodal hydropause.

It remains to be seen if it is true that the results obtained on simulated data carry on to actual measurements and whether the exploitation of the method presented here can be helpful in an operational mode.

This work can be improved in many respects, however we believe that the next step to be taken is the test of the method presented on real data.

## REFERENCES

- ALUFFI-PENTINI F., PARISI V. and ZIRILLI F., *A global optimization algorithm using stochastic differential equations*, *Trans. Math. Soft. ACM*, **14** (1988a) 345-366.
- ALUFFI-PENTINI F., PARISI V. and ZIRILLI F., *Algorithm 667 SIGMA-A stochastic integration global minimization algorithm*, *Trans. Math. Soft. ACM*, **14** (1988b) 366-380.
- BEVIS B. G., BUSSINGER S., HERRING T. A., ROCKEN C., ANTHES R. A. and WARE R. H., *GPS Meteorology: Remote Sensing of Atmospheric Water Vapour Using the Global Positioning System*, *J. Geophys. Res.*, **97** (1992) 15787-15801.
- ELLINGSON R. G. and FOUQUART Y., *The intercomparison of radiation codes in climate models: an overview*, *J. Geophys. Res.*, **96** (1991) 8925-8927.
- HARDY K. R. *et al.*, *Atmospheric profiles from active space-based radio measurements*, *Conference on Satellite Meteorology and Oceanography, January 5-10, 1992, Atlanta, GA* (American Meteorological Society, Boston, Mass) 1992.
- HARRIES J. E., *The greenhouse earth: a view from space*, *Quart. J. R. Met. Soc.*, **122** (1996) 799-818.